

Energy- and angle-resolved measurements of the Rh(${}^4F_{9/2}$) and Rh(${}^4F_{7/2}$) populations from ion bombarded Rh{100}

N. Winograd, M. El-Maazawi, R. Maboudian, Z. Postawa,^{a)} D. N. Bernardo,
and B. J. Garrison

Department of Chemistry, The Pennsylvania State University, University Park, Pennsylvania 16802

(Received 29 November 1991; accepted 10 February 1992)

The measurement of the energy and the angular distributions of excited atoms desorbed from ion-bombarded solids has been of long-standing interest since these distributions hold the key to understanding the excitation and deexcitation processes. Although many investigators have experimentally determined the energy distributions of atoms ejected in various excited states, all these measurements have been confined to a single angle of emission.¹ Corresponding theories and models have thus concentrated on the velocity dependence of the excitation probability. In 1954, Hagstrum proposed that for excited atom fractions, the velocity dependence of the excitation probability should follow an $\exp(-A/av_1)$ behavior, where v_1 is the component of escape velocity perpendicular to the surface and A/a is the deexcitation coefficient.² This relation has been used to describe experimental distributions except for the low velocity regime where surface binding energy effects are suggested to alter this dependence.³⁻⁵

In this Communication, we present energy- and angle-resolved neutral (EARN) distributions of excited Rh atoms (${}^4F_{7/2}$ state, with excitation energy of 0.2 eV) ejected from Rh{100} by bombardment with a 5 keV Ar⁺ ion beam at normal incidence. In addition, we have measured the EARN distributions of atoms in the ${}^4F_{9/2}$ ground state. In this way, for the first time the final excitation probability can be presented as a function of the emission velocity and the take-off angle of the particles. These results show that at high velocities, the dependence is indeed $\exp(-A/av_1)$, although the value of A/a changes by over 50% depending on the polar and azimuthal angles of detection. Moreover, at lower velocities, the ratio becomes almost independent of velocity. We show that collisional excitation and the details of individual atomic motions are needed to account for the details of the velocity and angular dependences of the excitation probability.

The EARN distributions have been obtained using a multiphoton resonance ionization (MPRI) scheme that has been described in detail elsewhere.^{6,7} A 200 ns pulse of 5 keV Ar⁺ ions is first focused at normal incidence onto a 2 mm spot on the sample. A given time ($> 1.5 \mu\text{s}$) after the ion impact, a ribbon-shaped laser pulse is used to resonantly ionize a small volume of the desorbed species. This time delay determines the velocity time-of-flight (TOF) of the probed species. Once the particles are ionized, they are accelerated toward a position-sensitive microchannel plate where they are detected. For a given azimuthal angle (φ), 30 images each corresponding to a different TOF are col-

lected, and sorted into an intensity map of kinetic energies (E) and take-off angles (θ).

The energy- and angle-resolved distributions of Rh atoms sputtered in the ground state and the next higher-lying excited state are presented in Fig. 1. The results correspond to ejection along two crystallographic directions, as defined in the inset to Fig. 1. For the ground state distribution, the most intense peak is seen along the $\varphi = 0^\circ$ azimuth ($\langle 100 \rangle$ direction) at a polar angle of about 50° . The observed angular anisotropies are the same as has been reported previously for the ground state.⁸ The EARN distributions of excited atoms are qualitatively different from the ground state distributions. First, the most intense peak appears at normal ejection ($\theta = 0^\circ$). Second, at low energies, only a shoulder exists along the $\varphi = 45^\circ$ azimuth ($\langle 110 \rangle$ direction). Third, the off-normal peak position occurs closer to the surface normal for the excited state than for the ground state. Fourth, the fall off with energy is much slower for the excited state.⁷

The relative populations in the ${}^4F_{9/2}$ and ${}^4F_{7/2}$ states was approximately 20 to 1. Our probing of the next higher-lying excited state (${}^4F_{5/2}$ with excitation energy of ~ 0.3 eV above the ground state) revealed its population to be at least two orders of magnitude smaller than that of the ${}^4F_{7/2}$ state. Since the population density of a given level has been found experimentally to exponentially decrease with the excitation energy,⁹ we conclude that the populations in the ground and first excited state are not affected by decay in the gas phase from higher excited states.

The observation that the population in the ground state is much larger than the excited states allows us to approximate the excitation probability by the ratio of the excited state to ground state distributions, $(dN^*/dv)/(dN/dv)$, rather than by the ratio of the excited state population to the total population. Since the excitation probability is generally thought to vary as $\exp(-A/av_1)$,^{2,10} we have plotted $(dN^*/dv)/(dN/dv)$ vs $1/v_1$ in Fig. 2 for several representative angles of ejection.

There are several features that are clear from inspection of Fig. 2. First, at high velocities the ratio exhibits the expected $\exp(-A/av_1)$ dependence. However, the value of A/a varies from 0.58×10^6 to 1.52×10^6 cm/s. Second, at low velocities there is a sharp leveling off of the intensity ratios. The height of this plateau depends strongly on the polar and azimuthal angles of ejection. A somewhat similar behavior has been observed and attributed to the effect of surface binding energy.³⁻⁵ However, in the present investigation, the deviation at low velocities occurs much more

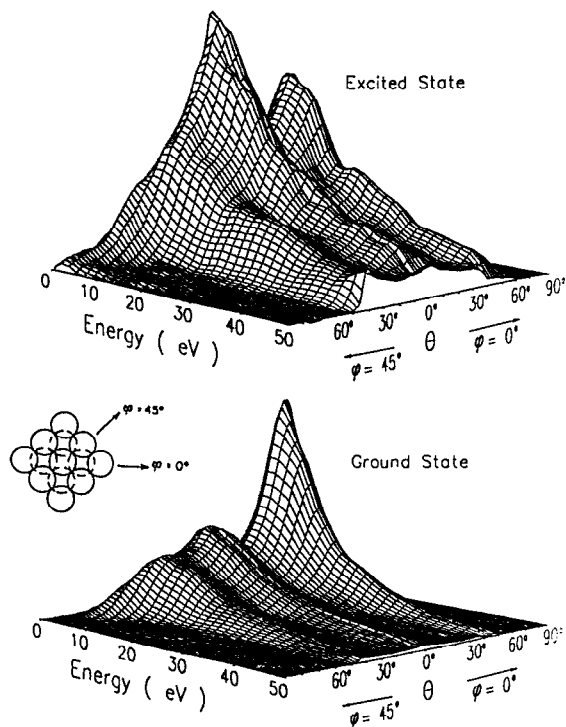


FIG. 1. Energy- and angle-resolved distributions of Rh atoms in the ${}^4F_{7/2}$ excited state and ${}^4F_{9/2}$ ground state, ejected from 5 keV Ar^+ ion bombarded $\text{Rh}\{100\}$. The data correspond to ejection along $\varphi = 0^\circ$ ($\langle 100 \rangle$) and $\varphi = 45^\circ$ ($\langle 110 \rangle$) crystallographic directions, as defined in the inset. Due to the symmetry of the surface and the angular resolution (e.g., $\Delta\varphi = \pm 18^\circ$ at $\theta = 45^\circ$), the results represent the data over $\sim 50\%$ of all space. Both plots are normalized to the maximum intensity peaks. The dashed circles in the inset represent second layer atoms.

abruptly, suggesting the existence of an additional excitation mechanism.¹¹

It is apparent that the simple exponential form of de-excitation works reasonably well in describing the major features of our experimental data. However, there is a richness in the discrepancies that we would like to explore further. These discrepancies may be tied to atomic motions that depend on the structure of the target and the trajectories of the ejecting atoms. To study the ejection and excitation processes on a microscopic scale, we have combined an electronic excitation model with our molecular dynamics procedure for calculating the motion of atoms during the keV particle bombardment process. To describe the excitation process, we use the kinetic ion emission model, which has previously been employed to describe collision-induced core excitations in aluminum.^{12,13} Unlike more recent and detailed excitation models, this procedure is easily incorporated into our molecular dynamics simulations. This allows us to examine the atomic collision sequences accompanying the excitation events. Moreover, it is possible to calculate the number of excited and ground state species that eject as a function of energy and angle, and compare the resulting distributions to the experimental ones.

The excitation mechanism in the kinetic ion emission model is based on the idea that when the distance between

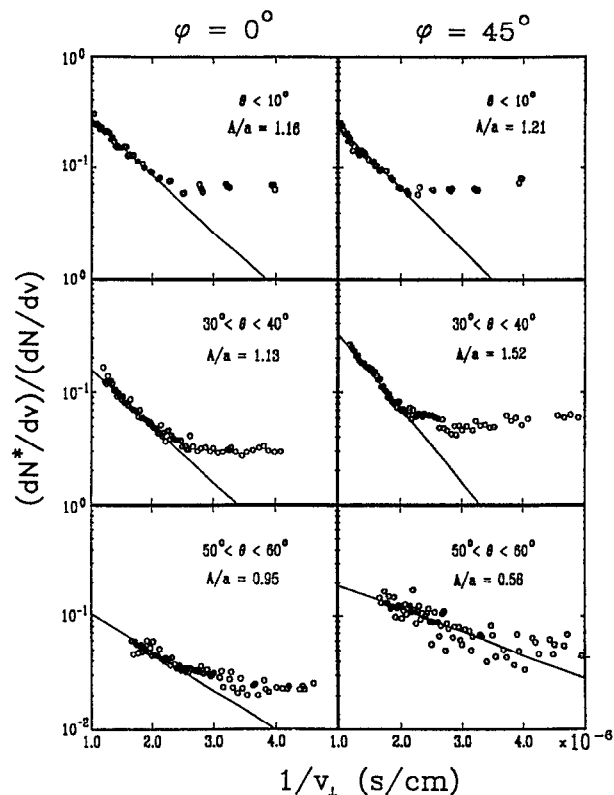


FIG. 2. Ratio of the measured intensities, $(dN^*/dv)/(dN/dv)$, vs $1/v_{\perp}$ for different angles of ejection. The data are direct ratios of the intensities given in Fig. 1. The straight lines displayed have been fit to the high velocity portions of the data and have slopes, A/a (in units of 10^6 cm/s).

two atoms in the solid approaches a threshold value, r_{th} , both atoms are excited with excitation probability P_0 . After this collision, the excitation can decay with some lifetime τ . The lifetime is assumed to have a constant value τ_s for $z < z_s$, where the height z is measured with respect to the original plane of surface atoms. For $z > z_s$, the lifetime is obtained from $1/\tau = (1/\tau_s)\exp[-\gamma(z-z_s)]$. For the calculations presented here, we have performed 4000 trajectories of 3 keV Ar^+ ions bombarding the $\text{Rh}\{100\}$ surface of a 867 atom target. The details are presented elsewhere.¹⁴

The results of the simulations are shown in Fig. 3 for atoms ejected with $\theta < 30^\circ$. Excitation probabilities of individual atoms are shown in Fig. 3(a). Most of the points are scattered about an exponentially decaying excitation probability on $1/v_{\perp}$. The large spread observed in the individual excitation probabilities is because each atom has a different history of collisional motion, initial excitation, and subsequent relaxation, thus resulting in different final excitation probabilities. We consider the average, P_{ave} , of these individual excitation probabilities to be proportional to the excited state population and $(1-P_{ave})$ to be proportional to the ground state population, since in the simulations we assume that the system contains only these two levels. Using these relations, one can predict the observed ratio of intensities by $(dN^*/dv)/(dN/dv) = P_{ave}/(1-P_{ave})$. This factor is displayed in Fig. 3(b). The calculated distribution

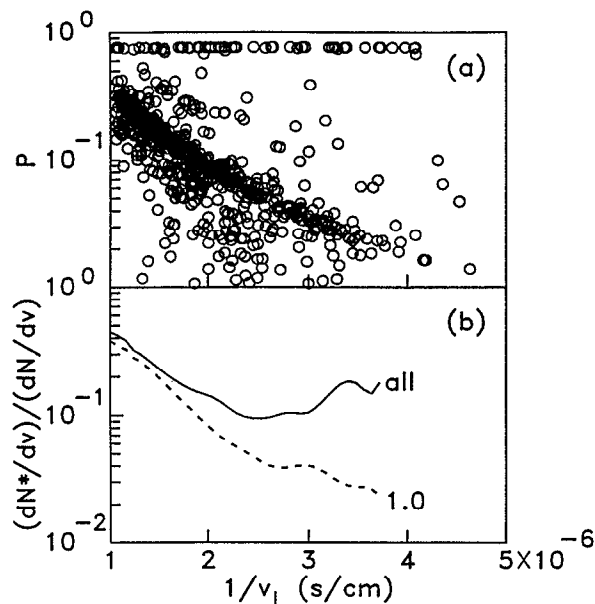


FIG. 3. Results of simulations. (a) Calculated excitation probabilities, P , of individual atoms vs $1/v_{\perp}$ for $\theta < 30^\circ$. (b) Ratio of intensities $(dN^*/dv)/(dN/dv)$ as obtained from the averaged excitation probability. The solid line includes all sputtered atoms whereas the dashed line represents the results for which atoms excited more than 1 \AA above the surface are excluded. The values of the parameters used are $P_0 = 0.76$, $r_{th} = 1.85 \text{ \AA}$, $\tau_s = 8.16 \text{ fs}$, $\gamma = 1.82 \text{ \AA}^{-1}$, and $z_s = 1.2 \text{ \AA}$ (see text for description). Since several thousand trajectories are required to obtain good statistics, no exhaustive optimization of the parameters has been attempted.

looks strikingly similar to the experimental one. In particular, the calculated distribution exhibits an $\exp(-A/av_{\perp})$ dependence at high velocities and an independence on velocity at low velocities.

Insight into the low-velocity behavior of the excitation probability can be gained by examining the individual atomic excitation probabilities as shown in Fig. 3(a). As mentioned earlier, most of the excitation probabilities are exponentially decaying with $1/v_{\perp}$. However, there exist ejected atoms whose excitation probabilities are quite high with practically no velocity dependence. The excitation history of these atoms can be examined using our molecular dynamics simulations, and we find that these atoms have been last excited by collisions with other atoms some distance ($1\text{--}20 \text{ \AA}$) above the surface.¹⁵ Within the framework of the model, these atoms are removed from interaction with the substrate, and thus their lifetimes are much longer. If the value of $(dN^*/dv)/(dN/dv)$ is recalculated excluding the atoms that are last excited above 1 \AA , a plateau is no longer observed at low velocities, as is shown in Fig. 3(b). The expected exponential dependence on $1/v_{\perp}$ becomes apparent. The enhanced excitation probability in the low velocity regime arises from the atoms that are excited above the surface and simply do not decay or deexcite. Since slow moving atoms that are excited at the surface almost completely deexcite, the atoms excited above the surface contribute significantly to the total excitation probability in the low velocity region. This produc-

tion of atoms excited $1\text{--}20 \text{ \AA}$ above the surface was observed in simulations involving a range of calculational parameters. For example, qualitatively similar results to those shown in Fig. 3(b) for Rh{100} were also found for Rh{111}.¹⁶ For the latter surface, a value of r_{th} equal to 1.46 \AA , in addition to 1.85 \AA , was tested. A lower value of r_{th} would, of course, make collisions over the surface even less probable.

It is worth noting that even when the atoms excited above the surface are removed from the calculations, the resulting $(dN^*/dv)/(dN/dv)$ ratio still has a slight curvature. Our analysis indicates that this gradual deviation is due to the effect of the surface binding energy.¹⁴ Hence, the surface binding energy alone cannot account for the abrupt leveling off of $(dN^*/dv)/(dN/dv)$ observed at low ejection velocities.

The other remarkable feature of our data is the fact that the ratio A/a depends on the polar and azimuthal angles of ejection. In the original Hagstrum model, this ratio was assumed to be a property of the system, and was taken to be a constant. Although the statistics in our calculation are not sufficiently good to look for these angular variations, analysis of the simulations indicates two possible mechanisms leading to an angle-dependent deexcitation coefficient. The first is due to the nonplanar nature of the surface binding energy⁸ which an atom must overcome before it ejects. Two atoms that eject at different angles can have different trajectory histories and different final excitation probabilities yet emerge with the same final value of v_{\perp} . Second, at high energies and off-normal angles ($\theta > 30^\circ$), an exiting atom can get reexcited via a collision with a neighboring atom. This leads to greater excitation probabilities at high velocities and a steeper high-energy slope (greater value of A/a).¹⁴

In conclusion, we have presented energy- and angle-resolved distributions of atoms in excited and ground states that are ejected from an ion-bombarded single crystal surface. By using molecular dynamics simulations in conjunction with the kinetic ion emission model, we can explain many of the important qualitative features of the data. It is conclusively shown that details of the atomic motions are important in understanding the features of the excited state distributions.

We gratefully acknowledge the financial support of the National Science Foundation, the Office of Naval Research, and the IBM Program for the Support of the Materials and Processing Sciences. Z. P. would like to thank the Polish Ministry of National Education Grant No. P/04/238 for additional support. The Pennsylvania State University supplied a generous grant of computer time for these studies.

^{a)}Permanent address: Institute of Physics, Jagellonian University, ulica Reymonta 4, PL-30-059 Kraków 16, Poland.

¹G. Betz, Nucl. Instrum. Methods B 27, 104 (1987), and references therein.

²H. D. Hagstrum, Phys. Rev. 96, 336 (1954).

³M. L. Yu and N. D. Lang, Phys. Rev. Lett. 50, 127 (1983).

⁴N. D. Lang, Phys. Rev. B 27, 2019 (1983).

⁵J. H. Lin and B. J. Garrison, J. Vac. Sci. Technol. A 1, 1205 (1983).

- ⁶P. H. Kobrin, G. A. Schick, J. P. Baxter, and N. Winograd, *Rev. Sci. Instrum.* **57**, 1354 (1986).
- ⁷M. El-Maazawi, R. Maboudian, Z. Postawa, and N. Winograd, *Phys. Rev. B* **43**, 12078 (1991).
- ⁸R. Maboudian, Z. Postawa, M. El-Maazawi, B. J. Garrison, and N. Winograd, *Phys. Rev. B* **42**, 7311 (1990).
- ⁹G. E. Young, M. F. Calaway, M. J. Pellin, and D. M. Gruen, *J. Vac. Sci. Technol. A* **2**, 693 (1984).
- ¹⁰M. L. Yu, D. Grischkowsky, and A. C. Balant, *Phys. Rev. Lett.* **48**, 427 (1982).
- ¹¹W. Heiland, J. Kraus, S. Leung, and N. H. Tolk, *Surf. Sci.* **67**, 437 (1977).
- ¹²J. J. Vrakking and A. Kroes, *Surf. Sci.* **84**, 153 (1979).
- ¹³M. H. Shapiro and J. Fine, *Nucl. Instrum. Methods B* **44**, 43 (1989).
- ¹⁴D. N. Bernardo, M. El-Maazawi, R. Maboudian, Z. Postawa, N. Winograd, and B. J. Garrison (manuscript in preparation).
- ¹⁵The height at which an atom is reexcited, z_r , is the subject of another study. We find that 50% of the reexcited atoms have $1 \text{ \AA} < z_r < 3.5 \text{ \AA}$, and 90% of the reexcited atoms have $1 \text{ \AA} < z_r < 9 \text{ \AA}$.
- ¹⁶D. N. Bernardo and B. J. Garrison (unpublished results).

*